The SAS model: A turbulence model with controlled modelled dissipation

Lars Davidson
Division of Fluid Dynamics
Department of Applied Mechanics
Chalmers University of Technology, Gothenburg, Sweden
web: www.tfd.chalmers.se/˜lada

Summary The SAS model (Scale Adapted Simulation) was invented by Menter and co-workers [1]. The idea behind the SST-SAS $k-\omega$ model is to add an additional production term — the SAS term — in the ω equation, which is sensitive to resolved (i.e. unsteady) fluctuations. When the flow equations resolve turbulence, the length scale based on velocity gradients is much smaller than that based on time-averaged velocity gradients. Hence the von Kármán length scale, L_{vK}, is an appropriate quantity to use as a sensor for detecting unsteadiness. In regions where the flow is on the limit of going unsteady, the objective of the SAS term is to increase ω. The result is that k and ν_t are reduced so that the modelled dissipation (i.e. the damping effect) of the turbulent viscosity on the resolved fluctuations is reduced, thereby promoting the momentum equations to switch from steady to unsteady mode.
The SST-SAS model and the standard SST-URANS are evaluated for developing channel flow. Unsteady inlet boundary conditions are prescribed in all cases by superimposing turbulent fluctuations on a steady inlet boundary velocity profile.

The Turbulence Model

The constitutive model for the turbulent Reynolds stresses — the Boussinesq assumption — which is used in the Navier-Stokes equations reads

$$\tau_{ij} = -2\nu_t \bar{s}_{ij} + \frac{2}{3}\delta_{ij}k, \quad \bar{s}_{ij} = \frac{1}{2}\left(\frac{\partial \bar{u}_i}{\partial x_j} + \frac{\partial \bar{u}_j}{\partial x_i}\right), \quad \varepsilon_M = -\tau_{ij}\frac{\partial \bar{u}_i}{\partial x_j} = 2\nu_t \bar{s}_{ij}\bar{s}_{ij} \tag{1}$$

where the continunity equation, $\partial \bar{u}_i/\partial x_i = 0$, was used in the last equality. The SST-SAS turbulence model reads

$$\begin{aligned}
\frac{\partial k}{\partial t} + \frac{\partial}{\partial x_j}(\bar{u}_j k) &= \frac{\partial}{\partial x_j}\left[\left(\nu + \frac{\nu_t}{\sigma_k}\right)\frac{\partial k}{\partial x_j}\right] + P_k - \beta^* k\omega \\
\frac{\partial \omega}{\partial t} + \frac{\partial}{\partial x_j}(\bar{u}_j \omega) &= \frac{\partial}{\partial x_j}\left[\left(\nu + \frac{\nu_t}{\sigma_\omega}\right)\frac{\partial \omega}{\partial x_j}\right] - \beta\omega^2 + C_\omega + \alpha S^2\left(1 + \underline{P_{SAS}}\right) \\
\nu_t \propto \frac{k}{\omega}, \quad & P_{SAS} = \tilde{\zeta}_2 \kappa \frac{L}{L_{vK,3D}}, \quad L_{vK,3D} = \kappa \frac{S}{U''},
\end{aligned} \tag{2}$$

where S and U'' are generic first and second velocity derivatives, respectively. The additional term in the SAS model is the underlined P_{SAS} term in the ω equation.

The source term, P_{SAS}, includes the second velocity gradient. This is interesting because the von Kármán length scale decreases when the momentum equations resolve (part of) the turbulence. The von Kármán length scale is smaller for an instantaneous velocity profile than for a time-averaged velocity, see Fig. 1. When making unsteady simulations, the momentum equations are triggered through instabilities to go unsteady in regions

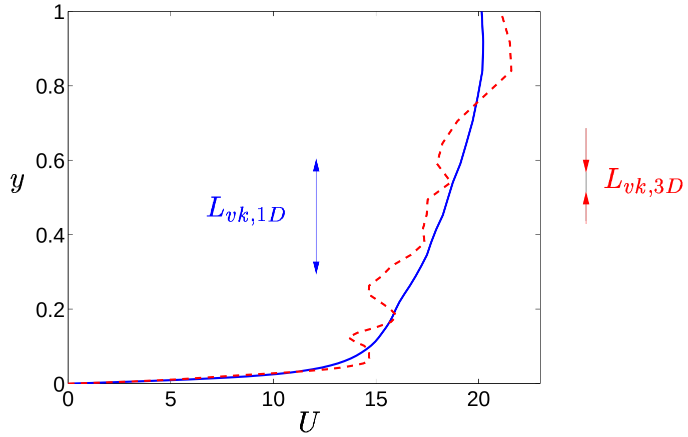

Figure 1: Velocity profiles from a DNS of channel flow. Solid line: time-averaged velocity with length scale $L_{vk,1D}$; dashed line: instantaneous velocity with length scale $L_{vk,3D}$.

where the grid is fine enough. With traditional turbulence models, high turbulent viscosity dampens out these instabilities. In many cases this is an undesired feature, because, if the flow wants to go unsteady, it is usually a bad idea to force the equations to stay steady. One reason is that there may not be any steady solution. Hence, the equations will not converge. Another reason is that, if the numerical solution wants to go unsteady, the large turbulent scales will be resolved instead of being modelled. This leads to a more accurate prediction of the flow.

The function of the SAS term in Eq. 2 acts as follows: in regions of fine grid, resolved unsteadiness will appear. This gives a small $L_{vK,3D}$ and hence — through P_{SAS} — a large ω which gives a reduced k and ν_t and a reduced modelled dissipation, ε_M. Hence the resolved unsteadiness is not dampened, but instead part of the turbulence is resolved. This gives an increased accuracy since a smaller part of the turbulence is modelled.

In traditional turbulence models the opposite happens: when in regions of fine grid, resolved unsteadiness appears, the production term P_k increases which results in an increased turbulent viscosity. The resolved unsteadiness and the result is a reduced accuracy. Also, as mentioned above, perhaps no converged solution will be obtained at all.

Evaluation of the von Kármán length scale in fully developed channel flow

In Fig. 2 different turbulent length scales are evaluated using DNS data of fully developed channel flow. Only viscous dissipation of resolved turbulence affects the equations in DNS. This implies that the smallest scales that can be resolved are related to the grid scale. The von Kármán length scale based on instantaneous velocities, $\langle L_{vK,3D}\rangle$, is shown in Fig. 2. For $y > 0.2$, its magnitude is close to Δy, which confirms that the von Kármán length scale is related to the smallest resolvable scales. Closer to the wall, $\langle L_{vK,3D}\rangle$ increases slightly while Δy continues to decrease.

The von Kármán length scale, $L_{vK,1D}$

$$L_{vK,1D} = \kappa \left| \frac{\partial \langle \bar{u} \rangle / \partial y}{\partial^2 \langle \bar{u} \rangle / \partial y^2} \right| \tag{3}$$

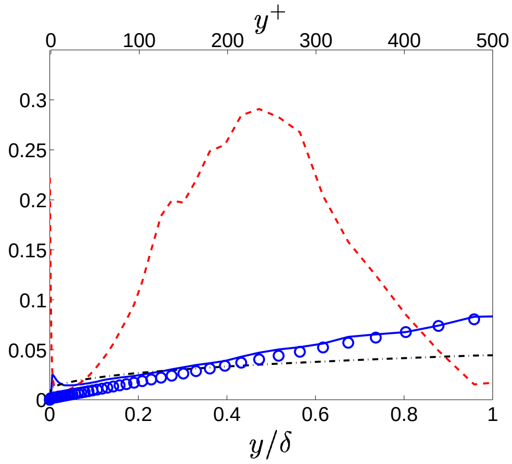

Figure 2: Turbulent length scales in fully developed channel flow. Left: global view; right: zoom. DNS. 96^3 mesh. $Re_\tau = 500$. $\Delta x/\delta = 0.065$, $\Delta z/\delta = 0.016$, y-stretching of 9%. —— : $\langle L_{vK,3D} \rangle$; - - - : $L_{vK,1D}$; - · - : $(\Delta x \Delta y \Delta z)^{1/3}$; o: Δy.

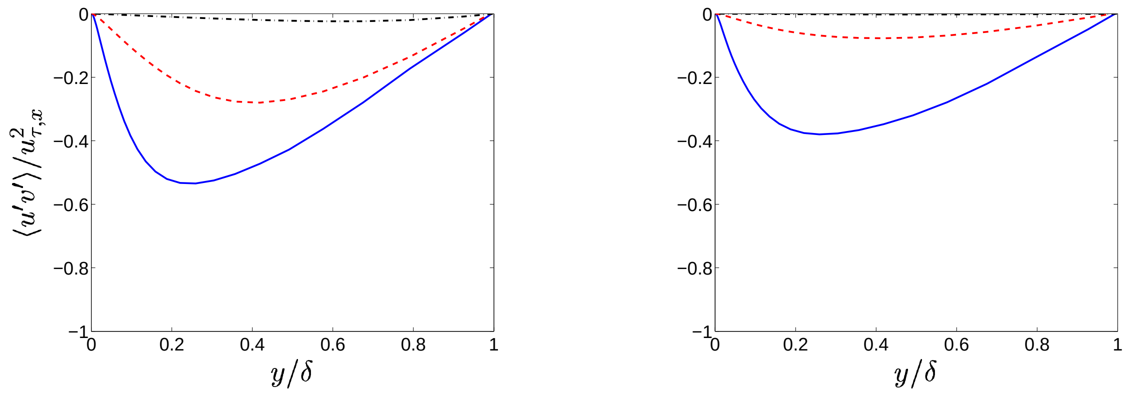

(a) SST-SAS.

(b) SST-URANS

Figure 3: Resolved shear stresses. —— : $x/\delta = 3.33$; - - - : $x/\delta = 23$; - · - : $x/\delta = 97$.

based on the averaged velocity profile, $\langle \bar{u} \rangle = \langle \bar{u} \rangle(y)$, is also included in Fig. 2 and, as can be seen, it is much larger than $\langle L_{vK,3D} \rangle$.

Near the wall, $L_{vK,1D}$ increases because the time-averaged second derivative, $\partial^2 \langle \bar{u} \rangle / \partial y^2$, goes to zero as the wall is approached. This behavior is not seen for the three-dimensional formulation, $\langle L_{vK,3D} \rangle$.

Results

A $256 \times 64 \times 32$ node mesh (x, streamwise; y, wall-normal; z, spanwise) was used. The size of the computational domain is $x_{max} = 100$, $y_{max} = 2$ (geometric stretching of 17%) and $z_{max} = 6.28$. This gives a Δx^+ and Δz^+ of approximately 785 and 393, respectively, and $y^+ < 1$ near the walls, expressed in inner scaling. In outer scaling, $\delta/\Delta x \simeq 2.5$ and $\delta/\Delta z \simeq 5$. The time step was set to $\Delta t u_\tau/\delta = 4.91 \cdot 10^{-3}$. The Reynolds number is $Re_\tau = u_\tau \delta/\nu = 2000$. Neumann boundary conditions are prescribed at the outlet.

The results using the standard SST-URANS model and the SST-SAS model are presented

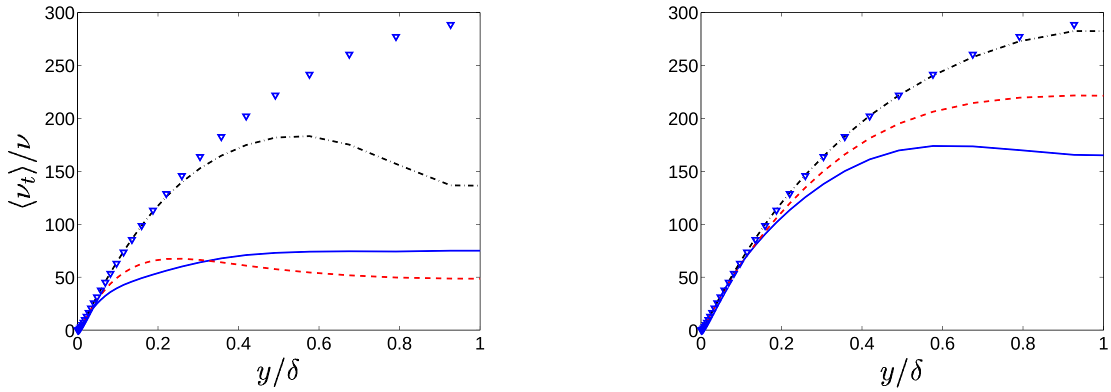

(a) SST-SAS.

(b) SST-URANS

Figure 4: Turbulent viscosity. —— : $x/\delta = 3.33$; - - - : $x/\delta = 23$; -·-·- : $x/\delta = 97$; $\triangledown$: from a 1D simulation with the SST model.

below. Figure 3 show the predicted resolved Reynolds shear stresses. As can be seen, the stresses predicted by the SST-SAS model decay at a slower rate than those predicted by the SST-URANS model. The reason is that the turbulent viscosity is smaller with the SST-SAS model than with the SST-URANS model (Fig. 4), which makes the dissipation of the resolved fluctuations smaller with the former model. It can be noted that, at the end of the channel ($x/\delta = 97$), the turbulent viscosity obtained with the SST-URANS model is equal to the turbulent viscosity predicted in a one-dimensional channel using the SST-URANS model (see Fig. 4b) and that the resolved stresses are zero. Hence, the flow has returned to fully steady conditions.

Conclusions

The SST-SAS model was compared with the standard SST-URANS model in channel flow. Unsteady, turbulent inlet boundary conditions are prescribed in both cases. It was confirmed that the SAS term acts as expected: it reduces the turbulent viscosity compared to the SST-URANS model and the resolved fluctuations are much larger with the SST-SAS model than with the SST-URANS model.

The SAS model and more results can be found in [2]

References

[1] F.R. Menter and Y. Egorov. A scale-adaptive simulation model using two-equation models. AIAA paper 2005–1095, Reno, NV, 2005.

[2] L. Davidson. Evaluation of the SST-SAS model: Channel flow, asymmetric diffuser and axi-symmetric hill. In *ECCOMAS CFD 2006*, September 5-8, 2006, Egmond aan Zee, The Netherlands, 2006 [1].

[1] can be downloaded from www.tfd.chalmers.se/~lada